JOURNAL OF COMPUTATIONAL PHYSICS 94, 138–150 (1991)

A Numerical Solution of the Steady Solidification Problem in Two Dimensions by Boundary-Fitted Coordinate Systems

MASATOSHI SAITOU, EIZABURO KANDA, AND MITSUO KAWASHIMA

Electronics Materials Laboratory, Sumitomo Metal Mining Co., Ltd., 1-6-1, Suehiro-cho, Ohme-Shi, Tokyo, 198, Japan

Received June 21, 1988; revised February 8, 1990

A simple numerical scheme is proposed to solve the problem of determining the interface shape under the thermal equilibrium condition. The procedure is based on a finite difference method using boundary-fitted coordinate systems. Several examples are given. This simple numerical solution method can be easily applied to any arbitrary shape and the unsteady solidification problem. © 1991 Academic Press, Inc.

INTRODUCTION

Many numerical solution methods have been developed in recent years to solve heat conduction equations with arbitrary shapes [1]. Knowledge of the solid–liquid interface, especially the control of the interface shape by the experimental parameters, is very important in determining the quality of the crystals [2].

Nash and Glicksman [3] calculated the solid–liquid interface in periodic grain boundaries by an integral method, taking both the steady-state heat conduction equation and the thermodynamic equation into account. But their method is complicated and limited to the boundary conditions. Other investigators have applied the numerical solution to the solidification problem [4, 5]. For example, under the condition that the interface shape was specified as parabolic [5], Navier–Stokes equations were solved numerically. However, the solid–liquid interface shape is not always parabolic in practice [6].

Though the analytical solutions are mainly for the one-dimensional cases of infinite or semi-infinite regions with simple boundary conditions [7], their solution methods have restrictions on their application.

This paper discusses the simple solution method of calculating the solid–liquid interface shape which satisfies both the steady state heat conduction and the thermodynamic equations. The discretization by the finite difference method is conducted in this method so as to ensure the second-order accuracy.

The use of the boundary-fitted coordinate system in this procedure is a very important element. This is because the boundary-fitted coordinate system easily enables us to calculate the grid points if the coordinates of the boundaries are given.

0021-9991/91 $3.00

Moreover, we use the *B*-spline function to represent the solid–liquid interface line and evaluate the derivatives at the interface.

To following section decribes the governing equations and the boundary conditions which are transformed to a general curvilinear coordinate. A simple numerical solution procedure is proposed.

GOVERNING EQUATIONS

The schematic diagram of the model solved in this paper is shown in Fig. 1. T_b and T_t are the temperature at the wall of the bottom and the top, m_S, m_L, and m_B are the temperature slope at the wall below the interface, above the interface, and at the wall of the bottom, respectively. For the temperature slope of the wall to be continuous at the interface, we use the interpolation by the quadratic curve.

As the growth process is governed by complex interactions between the velocity, temperature, and impurity concentration [8, 9], we simplify the governing equations by considering only the temperature field in the absence of buoyant convection fow and the segregation of impurities. Naturally the application is limited. However, we expect the basic understanding of the solidification process obtained to be useful in the case of considering the buoyant convection or the impurity concentration.

The growth rate in our paper is taken as zero because the Gibbs–Thompson relation [10] which is introduced in Eq. (3) is obtained from the thermal equilibrium condition.

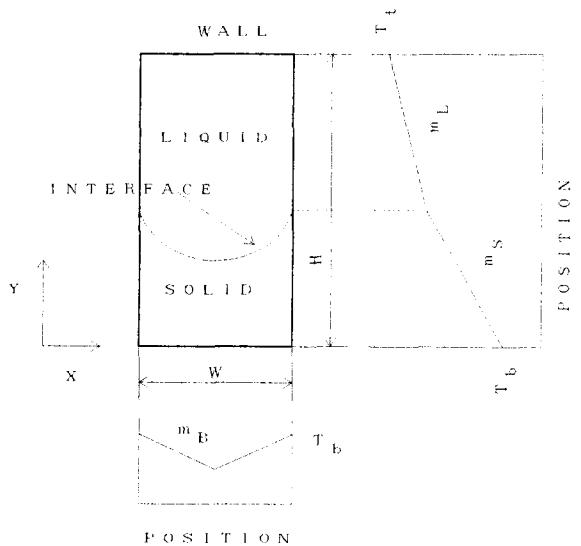

FIG. 1. Schematic representation of the solid–liquid interface.

Hence, the steady state heat conduction equation and the boundary condition at the interface can be written as

$$\nabla^2 T = 0, \tag{1}$$

$$\kappa_L \mathbf{n} \cdot \nabla T|_L = \kappa_S \mathbf{n} \cdot \nabla T|_S, \tag{2}$$

where T[K] is temperature, κ_L[W/cm K] is thermal conductivity in liquid, κ_S is that in solid, and $\mathbf{n}$ is the normal unit vector on the interface.

The Gibbs–Thompson relation provides the differential equation for the solid–liquid interface shape [10]. This equation can be written as

$$T_e = T_m[1 - \gamma/(Lr)], \tag{3}$$

$$r = -(1 + f'^2)^{3/2}/f'', \tag{4}$$

$$T_e \leqslant T_m, \tag{5}$$

where T_e[K] is the equilibrium temperature at the interface, T_m[K] is the melting temperature, γ[dyn/cm] is the surface energy, L[J/g] is the latent heat of fusion, r[cm] is the curvature radius, f' is the first derivative on x of the interface line $f(x)$, and f'' is the second derivative.

Equation (5) shows that only the supercooling is considered here. Therefore from Eqs. (3) and (5) we find the curvature to be positive.

Accordingly, the numerical solution of the solid–liquid interface should satisfy both Eqs. (1) and (3), as well as the Dirichlet boundary conditions on the walls.

Consider the boundary-fitted coordinate system [11, 12],

$$x = x(\xi, \eta), \qquad y = y(\xi, \eta), \tag{6}$$

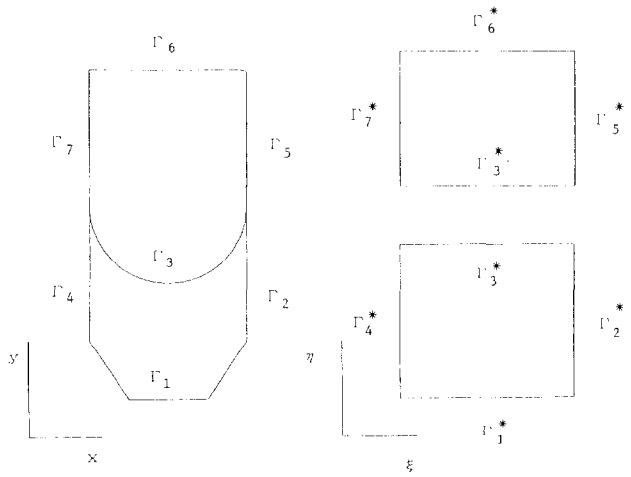

FIG. 2. A map of region at transformation.

defined as the solution of the quasi-elliptic equations,

$$\begin{aligned} g_{11}x_{\xi\xi} - 2g_{12}x_{\xi\eta} + g_{22}x_{\eta\eta} + J^2(Px_\xi + Qx_\eta) = 0, \\ g_{11}y_{\xi\xi} - 2g_{12}y_{\xi\eta} + g_{22}y_{\eta\eta} + J^2(Py_\xi + Qy_\eta) = 0, \end{aligned} \tag{7}$$

where

$$\begin{aligned} g_{11} &= x^2{}_\eta + y^2{}_\xi, \qquad g_{12} = x_\xi x_\eta + y_\xi y_\eta, \\ g_{22} &= x^2{}_\xi + y^2{}_\xi, \qquad J = x_\xi y_\eta - x_\eta y_\xi. \end{aligned} \tag{8}$$

$P(\xi, \eta)$ and $Q(\xi, \eta)$ are functions of the control of spacing of the coordinate lines.

The sketch in Fig. 2 illustrates the map transforming the physical plane (x, y) into a rectangular computational plane (ξ, η) with uniform grids. Equation (7) is solved by the SOR method [13]. A transformation example is shown in Fig. 3. The choice of the functions P and Q is in accordance with Ref. [13],

$$\begin{aligned} P &= -\sum_{i=1}^{n} a_i \operatorname{sgn}(\xi - \xi_i) \exp(-c_i |\xi - \xi_i|), \\ Q &= -\sum_{j=1}^{m} a_j \operatorname{sgn}(\eta - \eta_j) \exp(-c_j |\eta - \eta_j|), \end{aligned} \tag{9}$$

where n and m are the number of ξ and η lines, a_i and b_i being constant. These equations have the effect of attracting the $\xi =$ constant lines to the $\xi = \xi_i$ lines, and attracting $\eta =$ constant lines to the $\eta = \eta_j$ lines.

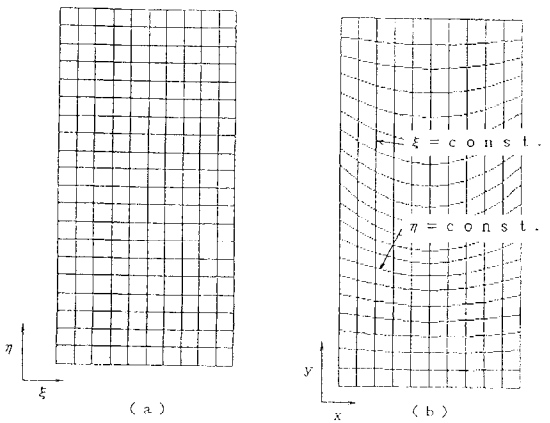

FIG. 3. Example of transformation. $P = 0$, $a_j = 0.1$, and $b_j = 0.2$ in Q when the attraction line index j is 11: (a) transformed plane with uniform grids; (b) physical plane.

Equations (1) and (2) are now transformed to the computational plane [11],

$$g_{11}T_{\xi\xi} - 2g_{12}T_{\xi\eta} + g_{22}T_{\eta\eta} + J^2(PT_\xi + QT_\eta) = 0, \tag{10}$$

$$\kappa_L \left.\frac{T_\xi(f'y_\eta + x_\eta) - T_\eta(f'y_\xi + x_\xi)}{J(1+f'^2)^{1/2}}\right|_L = \kappa_S \left.\frac{T_\xi(f'y_\eta + x_\eta) - T_\eta(f'y_\xi + x_\xi)}{J(1+f'^2)^{1/2}}\right|_S. \tag{11}$$

B-Spline Function and the Fitting of the Interface

Close attention should be paid to determining the derivatives f' and f'' in Eqs. (4) and (11); otherwise large numerical errors will be caused by the approximation errors of the derivatives. For example, f' is approximated by the use of the center difference formula,

$$f' = (f_{i+1,j} - f_{i-1,j})/2 + O(\Delta x^2). \tag{12}$$

The *B*-spline [14, 15] is superior to the above approximation because its slope and curvature are continuous at the junction points. However, if the Neumann or the periodical condition is given as the end condition, the cubic spline may be applied to the approximation of the interface line [16, 17]. Consider an interface that is represented by an ordered sequence of interface points,

$$(x_0, r(x_0)), (x_1, r(x_1)), \ldots, (x_N, r(x_N));$$

that is, a single value in x and $r(x_j)$ is the curvature radius at x_j. We present a method to locate the interface line $f(x)$, expanding $f'(x)$ by the truncated power function M_{mi} [14, 15],

$$f'(x) = \sum_{j=1}^{n+m} C_j M_{mj}(x), \tag{13}$$

where

$$M_{mj}(x) = M_m(x; \xi_{j-m}, \xi_{j-m+1}, \ldots, \xi_j) = \frac{M_m(x; \xi_{j-m+1}, \ldots, \xi_j) - M_m(x; \xi_{j-m}, \ldots, \xi_{j-1})}{\xi_j - \xi_{j-m}} \tag{14}$$

and

$$M_m(x; y) = (y-x)_+^{m-1} \begin{cases} (y-x)^{m-1}, & y \geqslant x \\ 0, & y < x. \end{cases} \tag{15}$$

One finds from the definition of M_{mj} that

$$M_{rj}(x)=\frac{(x-\xi_{j-r})\,M_{r-1\,j}(x)}{\xi_j-\xi_{j-r}}, \qquad r=2, 3, ..., m; \tag{16}$$

$$M_{1j}(x)=\begin{cases}(\xi_j-\xi_{j-1})^{-1}, & \xi_{j-1}\leqslant x<\xi_j\\ 0, & \xi_{j-1}>x,\ x\geqslant\xi_j.\end{cases} \tag{17}$$

Thus the knot values ξ_i should be taken as

$$\begin{gathered}x_i<\xi_{i+1}<x_{m+1}, \qquad i=0, 1, ..., n-1,\\ N+1=n+m,\end{gathered} \tag{18}$$

where $N+1$ is the number of sample points.

The derivatives of M_{rj} are obtained from Eqs. (16) and (17),

$$M'_{1j}(x)=0, \tag{19}$$

$$\begin{aligned}M'_{rj}=\{&M_{r-1\,j-1}(x)-M_{r-1\,j}(x)+(x-\xi_{j-r})\,M'_{r-1\,j-1}(x)\\ &+(\xi_j-x)\,M'_{r-1\,j}(x)\}/(\xi_j-\xi_{j-r}).\end{aligned} \tag{20}$$

The curvature radius can be written from Eqs. (4) and (13),

$$r(x_j)=-\frac{[1+(\sum_{i=1}^{n+m}C_iM_{mi}(x_j))^2]^{3/2}}{\sum_{i=1}^{n+m}C_iM'_{mi}(x_j)}. \tag{21}$$

Rewriting Eq. (21) and following Newton's method, we have a form of calculating C_i,

$$F^k{}_j+\sum_{j=1}^{n+m}\frac{\partial F^k{}_j}{\partial C_j}\Delta C^k_j=0, \tag{22}$$

$$C^k{}_j=C^k{}_j+\Delta C^k{}_j, \tag{23}$$

$$E=\sum_{j=1}^{n+m}|\Delta C^k{}_j|, \tag{24}$$

where k is the iteration cycle and

$$F^k{}_j=r(x_j)+\frac{[1+(\sum_{i=1}^{n+m}C_iM_{mi}(x_j))^2]^{3/2}}{\sum_{i=1}^{n+m}C_iM'_{mi}(x_j)}. \tag{25}$$

We can easily obtain the solution of Eq. (22), $C^k{}_j$, by Gauss's elimination method. The iteration is continued until $E=\sum_{j=1}^{n+m}|\Delta C^k{}_j|<\varepsilon$.

We have the integral form of Eq. (13),

$$f(x_{i+1}) - f(x_i) = \int_{x_i}^{x_{i+1}} \sum C_j M_{mj}(x)\, dx. \tag{26}$$

The right-hand term is calculated using the values of C_j, so we can obtain the value of $f(x)$ at x_j from Eq. (26) if the value of $f(x)$ at the end, x_0 or x_N, is given.

Discretization and Numerical Solution

The numerical algorithm for the solidification problem is formulated below. Equation (10) is approximated on the computational plane by the second-order central finite difference formulae and can be rewritten for the nth sweep,

$$\begin{aligned} T_{i,j}^{n+1} = T_{i,j}^{n} + \omega[&2(g_{11}+g_{22})\, T_{i,j}^{n} - g_{11}(T_{i+1,j}^{n} + T_{i-1,j}^{n+1}) \\ &- g_{22}(T_{i,j+1}^{n} + T_{i,j-1}^{n+1}) + g_{12}(T_{i+1,j+1}^{n} - T_{i+1,j-1}^{n+1} \\ &- T_{i-1,j+1}^{n} + T_{i-1,j-1}^{n+1})/2 - J^2\{P(T_{i+1,j}^{n} - T_{i-1,j}^{n+1}) \\ &- Q(T_{i,j+1}^{n} - T_{i,j-1}^{n+1})\}]/\{2(g_{11}+g_{22})\}, \end{aligned} \tag{27}$$

where ω is an acceleration parameter. As well known, the value of ω is very sensitive to the convergence rate, typically $\omega = 1.7$.

Equation (11) is approximated by the finite difference method,

$$\begin{aligned} T_{ei,j} = [&-(T_{i,j+2} - 4T_{i,j+1})(f'y_\xi + x_\xi)/2|_{\mathrm{L}} \\ &- R(T_{i,j-2} - 4T_{i,j-1})(f'y_\xi + x_\xi)/2|_{\mathrm{S}} \\ &+ (T_{i+1,j} - T_{i-1,j})\{-(f'y_\eta + x_\eta)|_{\mathrm{L}} \\ &+ R(f'y_\eta + x_\eta)|_{\mathrm{S}}\}/2]/[3\{(f'y_\xi + x_\xi)|_{\mathrm{L}} + R(f'y_\xi + x_\xi)|_{\mathrm{S}}\}/2], \end{aligned} \tag{28}$$

where

$$R = \kappa_{\mathrm{L}} J_{\mathrm{S}} / \kappa_{\mathrm{S}} J_{\mathrm{L}}.$$

Substituting the second-order difference equation below into Eq. (11) yields Eq. (28),

$$T_\eta|_{\mathrm{L}} = (-T_{i,j+2} + 4T_{i,j+1} - 3T_{i,j})/2 \tag{29}$$

and

$$T_\eta|_{\mathrm{S}} = (T_{i,j-2} - 4T_{i,j-1} + 3T_{i,j})/2. \tag{30}$$

Equation (27) can be solved by the use of the usual SOR.

The interface line $f(x_i)$ is determined by the following procedure:

(1) An unknown interface line and the unknown curvature radius are assumed to be $f^k{}_{i,h} = f^k(x_i)$ and $r^k{}_i(x_i)$, where k is the iteration number.

(2) The physical plane (x, y) is transformed to the computational plane (ξ, η). Equation (7) can be solved by the usual SOR method.

(3) Equations (27) and (28) give the temperature distribution under the assumption of procedure (1). The convergence condition is defined as

$$\sum_{i,j} |T^{n+1}{}_{i,j} - T^n{}_{i,j}| < \varepsilon_1, \tag{31}$$

typically $\varepsilon_1 = 1.0E\text{–}04$.

(4) The equilibrium temperature at the interface T_e is calculated from Eq. (3). Using the interface temperature T_{int} determined from procedure (3), we obtain the new radius $r^{k+1}{}_i$,

$$r^{k+1}{}_i = r^k{}_i + c(r_i - r^k{}_i), \tag{32}$$

where

$$r_i = \frac{\gamma}{L[1 - (T_e + T_{int})/2/T_m]}, \tag{33}$$

and $0 < c < 1$. Equation (33) is obtained from Eq. (3) by the replacement of T_e by $(T_{int} + T_e)/2$. We find C_j and the new interface $f^{k+1}{}_{i,h}$ from Eqs. (21)–(26).

(5) The thermal equilibrium interface line is determined from T_e and the temperature distribution calculated in procedure (3). The interface line obtained is taken as $f^{k+1}{}_{i,t}$.

(6) A parameter E characterizing the convergence can be defined:

$$E = \sum_i |f^{k+1}{}_{i,h} - f^{k+1}{}_{i,t}|. \tag{34}$$

The iteration procedure is continued until the convergence criterion

$$E < \varepsilon_2, \tag{35}$$

is satisfied, typically $\varepsilon_2 = 1.0E\text{–}0.4$.

Sample Applications

The simple numerical solution of this study can be applied to cases in the absence of free flow and solute segregation. Two examples are calculated, using personal computer PC-98XA. The interface shape is represented by the B-spline function with $m = 5$ and $N + 1 = 21$.

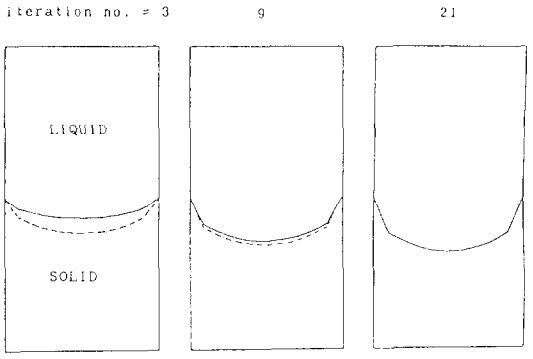

FIG. 4. Convergence process of the calculated interface: dashed curve—interface determined by the Gibbs–Thompson relation; full curve—interface determined by the steady-state heat conduction.

The convergence process of the assumed interface and the calculated interface is displayed in Fig. 4. In Fig. 4(c), the solid–liquid interface satisfies both requirements, i.e., the energy conservation and the thermodynamics.

The example in Fig. 5 shows that: (a) when $\kappa_S m_S < \kappa_L m_L$, the interface shape is concave toward the liquid; (b) when $\kappa_S m_S = \kappa_L m_L$, it is flat; and (c) when $\kappa_S m_S > \kappa_L m_L$, it is convex.

The interface temperature in this case is nearly equal to the melting temperature, so we apply the B-spline to $f(x)$ but not $r(x)$ and use the iteration procedure, $f^{k+1}{}_{i,h} = f^k{}_{i,h} + c(f^k{}_{i,h} - f^k{}_{i,t})$ instead of Eq. (32). The values of the parameters used for calculating are shown in Table I [18]. As only the ratio of thermal conductivity in the liquid and that in the solid is necessary for the calculation, no value of thermal conductivity is listed.

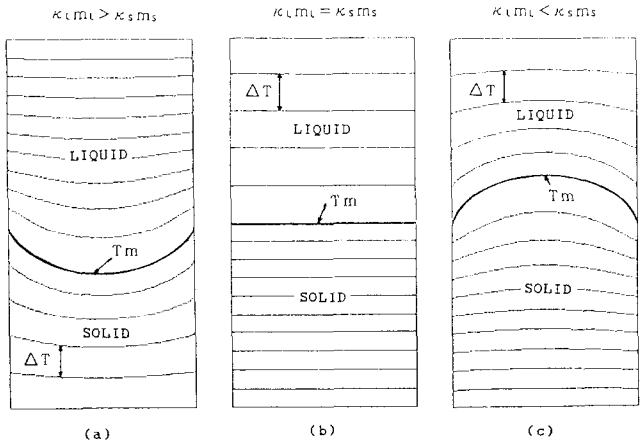

FIG. 5. Illustration of the isotherms and the solid–liquid interface (thick curve) for three types of $\kappa \cdot m$; $\Delta T = 1.0$K: (a) $\kappa_L m_L/\kappa_S m_S = 4.0$; (b) $\kappa_L m_L/\kappa_S m_S = 1.0$; (c) $\kappa_L m_L/\kappa_S m_S = 0.25$.

TABLE I

Values of Parameters Used in Calculations

Parameter / Figure	κ_L/κ_S	m_L[K/cm]	m_S[K/cm]	m_B[K/cm]	W[cm]	H[cm]
5.(a)	2	2	1	0	5	10
(b)	0.5	2	1	0	5	10
(c)	0.5	1	2	0	5	10
6	4	1	1	8	1	10
8.(a)	2	20	40	0	8×10^{-3}	10^{-2}
(b)	1	20	20	0	8×10^{-3}	10^{-2}
(c)	0.5	40	20	0	8×10^{-3}	10^{-2}

Note. Heat of fusion, L[J/g] = 726; surface tension, γ[dyn/cm] = 700; melting temperature T_m[K] = 1511.

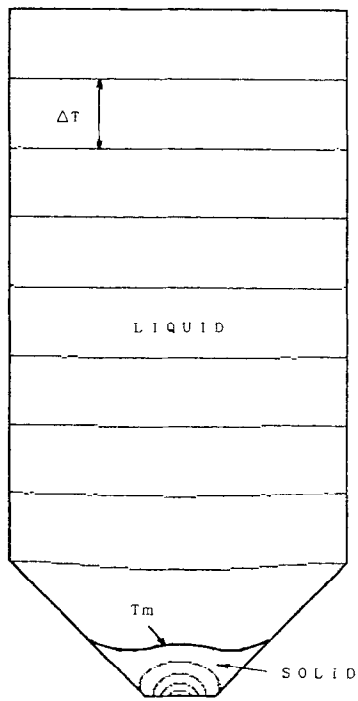

FIG. 6. Illustration of the isotherms and the solid–liquid interface (thick curve); $\Delta T = 1.0$K.

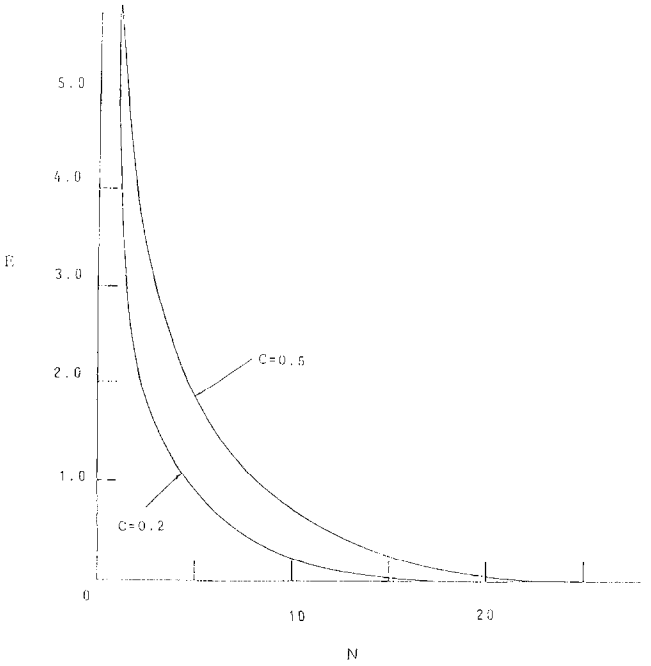

FIG. 7. Convergence history for two values of C: E: error norm; N: iteration cycles.

This criterion for the interface shape is physically justified in view of the thermal transport at the interface and is probably useful in practice. The detailed results will be reported elsewhere. The numerical procedure to determine the isothermal contours follows Thompson's method [13].

The example illustrated in Fig. 6 shows that the interface shape is not parabolic but like a letter "w" because of the bottom gradient m_B. We apply the B-spline to $f(x)$ but not to $r(x)$ because the interface temperature is nearly equal to the melting temperature. This calculated interface shape is qualitatively in agreement with the reported experiment [6]. The values of the parameters used for calculation are shown in Table I.

Calculation time is about 6–30 min. It is found that calculation time depends not on the transformation from the physical plane to the transformed plane but on the number of grid points. The two examples in this paper have 20×20 grid points in one region. The relationship between the convergence rate and C in Eq. (32) is shown in Fig. 7. It is found that the SOR is an effective and stable method of solving Eqs. (1), (2), and (3).

According to Nash and Glickman's model [3], we calculate the interface shape shown in Fig. 8 with the grain boundary present. The boundary conditions are: (1) $f'(x) = 1/\tan(\psi/2)$ at x_0; (2) $f'(x) = 0$ at x_N, where ψ is the contact angle between the two crystals. We solve Eq. (32) and the above boundary conditions

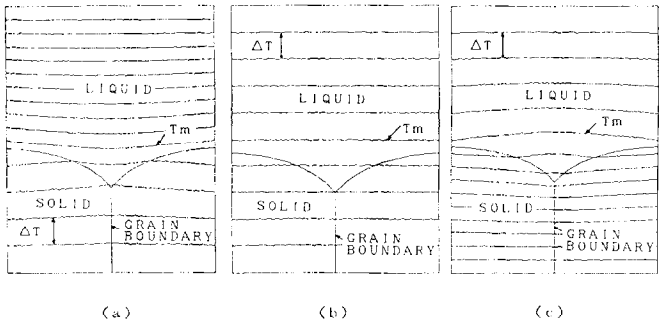

FIG. 8. Illustration of the isotherms and the solid–liquid interface showing the Gibbs–Thompson effect; $\Delta T = 0.02$K, $\psi = 80°$: (a) $\kappa_L/\kappa_S = 2$; (b) $\kappa_L/\kappa_S = 1$; (c) $\kappa_L/\kappa_S = 0.5$.

simultaneously to obtain C_j. The values of the parameters used are shown in Table I. The interface line is unequal to the melting temperature isotherm because of the Gibbs–Thompson effect. We assume the slight fluctuations of the isotherms in Fig. 8 are caused by the calculation errors. The accuracy of calculation would be improved by the increase of grid points.

In solving the steady solidification problem with the iterative procedure, it is very convenient that the grid points at the new step are automatically generated simply by lving Eq. (7). Undoubtedly it foes without saying that the initial guess must be within a certain neighborhood of the solution in Eq. (7), if the iterative solution is to converge. This is because Eq. (7) is nonlinear. Following Ref. [13], the weighted average of four boundary points is chosen as the method of making the initial guess. The simple numerical scheme presented here enables us to easily obtain the solid–liquid interface which satisfies both the heat conduction and thermodynamics. Problems with arbitrary shapes can also be solved. The solutions will be very useful in understanding crystal growth in a Bridgman method. With some minor modifications, the present scheme can be applied to the unsteady solidification problem.

REFERENCES

1. H. M. ETTOUNEY AND R. A. BROWN, *J. Comput. Phys.* **49**, 118 (1983).
2. F. R. SZOFRAN AND S. L. LEHOCZKY, *J. Cryst. Growth* **70**, 349 (1984).
3. G. E. HASH AND M. F. GLICKSMAN, *Philos. Mag.* **24**, 577 (1971).
4. T. JASINSKI AND A. F. WITT, *J. Cryst. Growth* **71**, 295 (1985).
5. F. M. CARLSON, A. L. FRIPP, AND R. K. CROUCH, *J. Cryst. Growth* **68**, 747 (1984).
6. A. TANAKA, Y. MASA, *et al.*, *Mat. Res. Soc. Symp. Proc.* **90**, 111 (1987).
7. J. CRANK, *Free and Moving Boundary Problems* (Oxford Science, London/New York, 1984).
8. C. J. CHANG AND R. A. BROWN, *J. Cryst. Growth* **63**, 343 (1983).
9. R. A. BROWN, *AIChE J.* **34**, 881 (1988).
10. D. P. WOODRUFF, *The Solid–Liquid Interface* (Cambridge Univ. Press, London/New York, 1973).
11. J. F. THOMPSON, Z. U. A. WARSI, AND C. W. MASTIN, *Numerical Grid Generation* (North-Holland, Amsterdam, 1985).

12. J. F. THOMPSON, F. C. THAMES, AND C. W. MASTIN, *J. Comput. Phys.* **24**, 274 (1977).
13. J. F. THOMPSON, F. C. THAMES, AND C. W. MASTIN, NASA CR-2729, 1976.
14. C. D. BOOR, *J. Approx. Theory* **6**, 50 (1972).
15. M. G. COX, *J. Inst. Math. Its Appl.* **10**, 134 (1972).
16. J. L. WALSH, J. H. AHLBERG, AND E. N. WILSON, *J. Math. Mech.* **11**, 225 (1962).
17. T. R. LUCAS, *SIAM J. Numer. Anal.* **11**, 569 (1974).
18. J. J. DERBY AND R. A. BROWN, *J. Cryst. Growth* **74**, 605 (1986).